Experimental Neurobiology
Vol. 19, pages 54~61, June 2010

Finger Motion Decoding Using EMG Signals Corresponding Various Arm Postures

Kyung-Jin You, Ki-Won Rhee and Hyun-Chool Shin*

Department of Electronic Engineering, College of IT, Soongsil University, Seoul 156-743, Korea

ABSTRACT

We provide a novel method to infer finger flexing motions using a four-channel surface electromyogram (EMG). Surface EMG signals can be recorded from the human body non-invasively and easily. Surface EMG signals in this study were obtained from four channel electrodes placed around the forearm. The motions consist of the flexion of five single fingers (thumb, index finger, middle finger, ring finger, and little finger) and three multi-finger motions. The maximum likelihood estimation was used to infer the finger motions. Experimental results have shown that this method can successfully infer the finger flexing motions. The average accuracy was as high as 97.75%. In addition, we examined the influence of inference accuracies with the various arm postures.

Key words: surface EMG, finger motions, neural signal processing, HCI

INTRODUCTION

Compared to the invasive type electromyogram (EMG) for measuring each motor unit action potential (MUAP) on muscle fiber in a small area, surface EMG signals can be recorded from the human body non-invasively and easily over wide skin areas. To extract the motion information, surface EMG signal processing has been studied, especially focusing on controlling electronic devices such as a human supporting prosthetic arms and smart interface (Sornmo and Laguna, 2005). Since motor commands are transmitted through internal nerve tissues or muscles, inferring such commands only from the surface EMG signals is not an easy task.

Thus many attempts to extract motor information from surface EMG have been made. A study of Englehart et al. (2001) used wavelet analysis and PCA analysis to classify two arm motions and two wrist motions. Also, Englehart and Hudgins (2003) used the absolute mean value, the zero crossing rate, and the wavelength to classify four arm and wrist motions. Momen et al. (2007) used RMS and FCMs to classify arm and wrist motions. Hudgins et al. (1993) obtained an ensemble average of EMG signals, and used a neural networks (NN) to classify four arm motions.

While the surface EMG-based motion inference has been focused on upper limb or hand motions, studies on inferring dexterous finger motions have not been done so much. Nishikawa et al. (1999) used the Gabor transform and absolute mean value to extract the features and classify four wrist motions and six finger motions in real-time learning

*To whom correspondence should be addressed.
TEL: 82-2-828-7165, FAX: 82-2-821-7653
e-mail: shinhc@ssu.ac.kr
Received June 15, 2010
Accepted for publication June 20, 2010

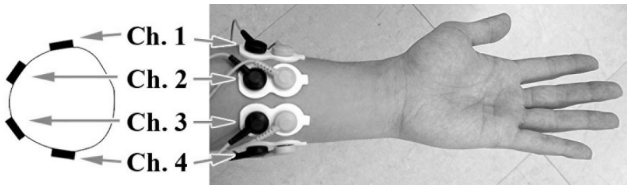

Fig. 1. Electrodes orientation for recording EMG on the forearm.

based on NN. Nagata et al. (2007) used absolute sum analysis, canonical component analysis, and minimum Euclidean distance to classify four wrist motions and five finger motions. Uchida et al. (1992) used FFT analysis and NN to classify four finger motions. Chen et al. (2007) used mean absolute values (MAV), the ratio of the MAVs, autoregressive (AR) model, and linear Bayesian classifier to classify 5∼16 finger motions. However, NN classifiers (Hudgins et al., 1993; Chen et al., 2007; Nagata et al., 2007) have strong dependency on initial parameter conditions. Also, linear classifiers (Uchida et al., 1992; Englehart et al., 2001; Englehart and Hudgins, 2003; Momen et al., 2007; Nagata et al., 2007) are simple but show low accuracy compared with nonlinear classifiers.

In this paper, we propose a novel method to infer the finger motions using surface EMG signals. We recorded the EMG signals during finger flexing motions. To infer the finger motions, we used the maximum likelihood method. The likelihood was obtained by building probabilistic models of EMG activities. The information entropy of the EMG magnitude was calculated to quantify the EMG activities. Experimentally we demonstrated that the proposed method could infer the finger flexing motions including multi-fingers as high as 97.75%.

In addition, we examined the influence of inference accuracies with various arm postures.

Multi-channel EMG recording

A signal acquisition device (Poly-G-A, Laxtha Inc., Korea), bi-polar Ag-AgCl electrodes (Dual electrode #272, Noraxon U.S.A. Inc.), and snap electrodes (SECS-4, Laxtha Inc., Korea) were used. The EMG signal was observed at the sampling frequency of 512 Hz and was filtered to reduce power line noise.

Two able-bodied subjects without any upper limb deficiencies participated in performing motions for this study and was trained before signal recording. The subjects were instructed to maintain their own flexing speed and strength.

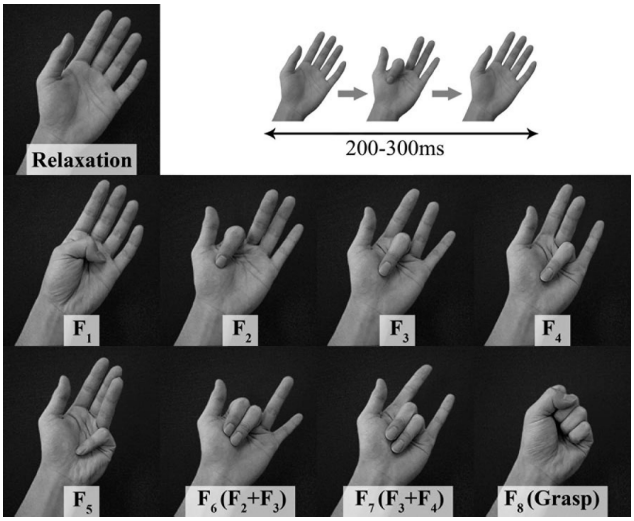

Fig. 2. Relaxation and finger flexing motions (F_1∼F_8).

The EMG signal was acquired with four channels on the left forearm (around the wrist) for 3.0 seconds. Fig. 1 shows electrode orientation for EMG recording. During the first 1.5 seconds, the subject did not perform any motion - termed 'relaxation' - and waited for an acoustic alarm. After 1.5 seconds, the subject heard the acoustic alarm and then flexed a finger immediately. After 3.0 seconds, the EMG signal recording procedure ended. In the experiment, the subject performed eight finger flexing motions including three multi-finger motions. Fig. 2 shows the detail of the finger motions. The subject took a long and sufficient rest between recording procedures to avoid muscle fatigue or cramp.

PROPOSED METHOD

Preprocessing of EMG signal

Here we consider four EMG channels and eight finger flexing motions. Let c and k be the channel and motion indexes, respectively. Then during F_k motion, the recorded raw EMG from the C^{th} channel can be denoted by $r_{k_c}[n]$ where n is a discrete time index.

Since the EMG signal has both positive and negative levels, we take an absolute of $r_{k_c}[n]$.

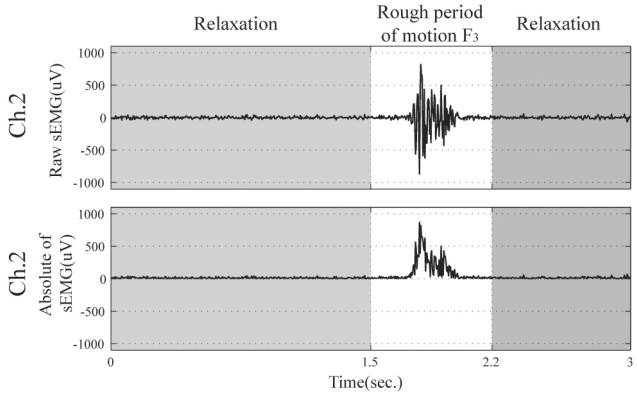

Fig. 3. Examples of raw EMG signal and absolute of EMG signal corresponding the 2nd channel during the F_3 motion. The recorded samples that treated as signals are limited in 1.5∼2.2 sec (unshaded area).

$$x_{k_c}[n] = |r_{k_c}[n]| \tag{1}$$

For example, Fig. 3 shows the surface EMG signal of the 2nd channel during the F_3 motions, $r_{3_2}[n]$ and $x_{3_2}[n]$.

Statistical EMG modeling

The amplitude of the EMG signal is a fundamental quantity which increases monotonically with the force developed in the muscle (Sornmo and Laguna, 2005). Moreover, the EMG signal represents a stochastic signal (Sornmo and Laguna, 2005).

The entropy (information entropy, H) was used to represent the characteristics of each EMG signal activity during finger flexing motions. The entropy is a measure that can reveal how much dynamical nature and the information (Shannon and Weaver, 1963) which the signal contains. Some EEG analysis methods based on entropy have been developed. (Capurro et al., 1999; Martin et al., 2000; Tong et al., 2002; Shin et al. 2006; Sabeti et al., 2009) Although the amplitude range or the spectral bandwidth of EMG and EEG signal are remarkably different, but they have a non- stationary stochastic property in common.

Conventionally the entropy is calculated as follows:

$$H(X) = \sum_{m=1}^{M} p(x_m)\log_2\frac{1}{p(x_m)} \tag{2}$$

where X denotes discrete random variable, $p(x_m)$ means the probability of the random variable X when X equals x_m and $\Sigma_{m=1}^{M} p(x_m) = 1$. For c^{th} channel and F_k motion, we define the probability $p_{k_c}(m)$ as

$$p_{k_c}(m) = \frac{\#\,\text{of samples} \in I_m}{\#\,\text{of total samples}},$$

$$I_m = \left\{ x_{k_c}[\,\cdot\,] | x_{\max}\frac{m-1}{M} \le x_{k_c}[\,\cdot\,] < x_{\max}\frac{m}{M} \right\},$$

$$m = 1, \ldots, M, \tag{3}$$

where M determines the number of total bins and $x_{\max}$ indicates the largest magnitude of the signal acquisition device. This value is set as $x_{\max} = 1{,}050\,\mu\text{V}$ in the study but can be adjusted to correspond to the subject's EMG characteristics. Then, the information entropy of the EMG signal is given by

$$H_{k_c} \equiv H(x_{k_c}) = \sum_{m=1}^{M} p_{k_c}(m)\log_2\frac{1}{p_{k_c}(m)}. \tag{4}$$

After accumulating the entropy in eq. (4), we build the probability density function of the entropy based on the Gaussian model:

$$f_{k_c}(h) = \frac{1}{\sqrt{2\pi\sigma_{k_c}^2}}\exp\left[-\frac{1}{2\sigma_{k_c}^2}\left(h-\mu_{k_c}\right)^2\right], \tag{5}$$

$$\mu_{k_c} = E\left[H_{k_c}\right],$$

$$\sigma_{k_c}^2 = E\left[\left(\mu_{k_c} - H_{k_c}\right)^2\right].$$

Here $f_{k_c}(h)$ is the probabilistic model based on the entropy of EMG signals. The example of this modeling is given in Fig. 4. Then we can get the probability density functions f_{k_c} on each channel for 8 different finger motions. Fig. 5 shows the resulting models of 8 finger motions and 4 channels. Assuming the statistical independence in each channel's EMG signal, the likelihood function $L(k)$ becomes

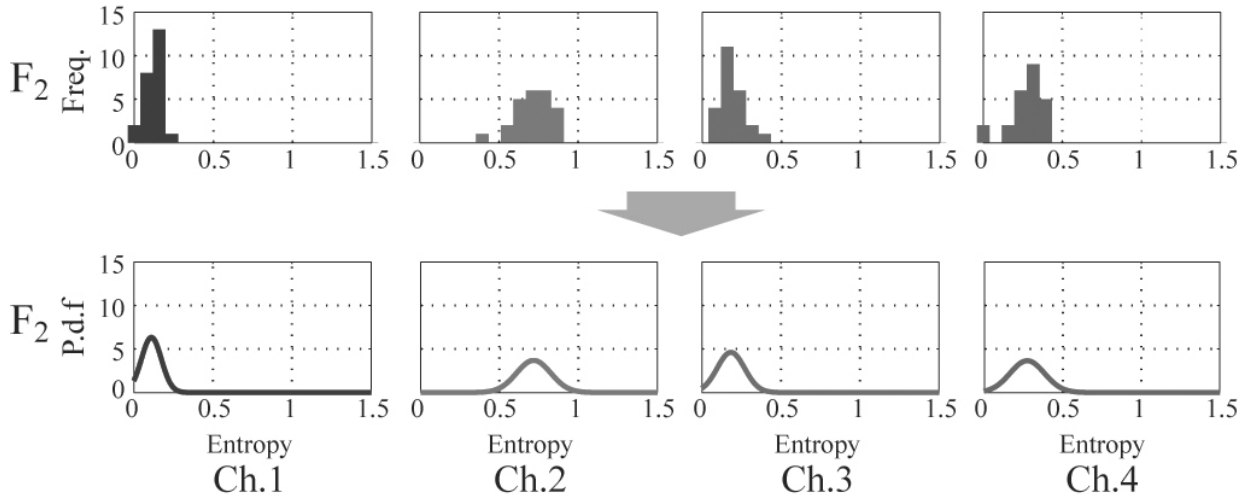

Fig. 4. Building the probabilistic model of the entropy of the EMG signals.

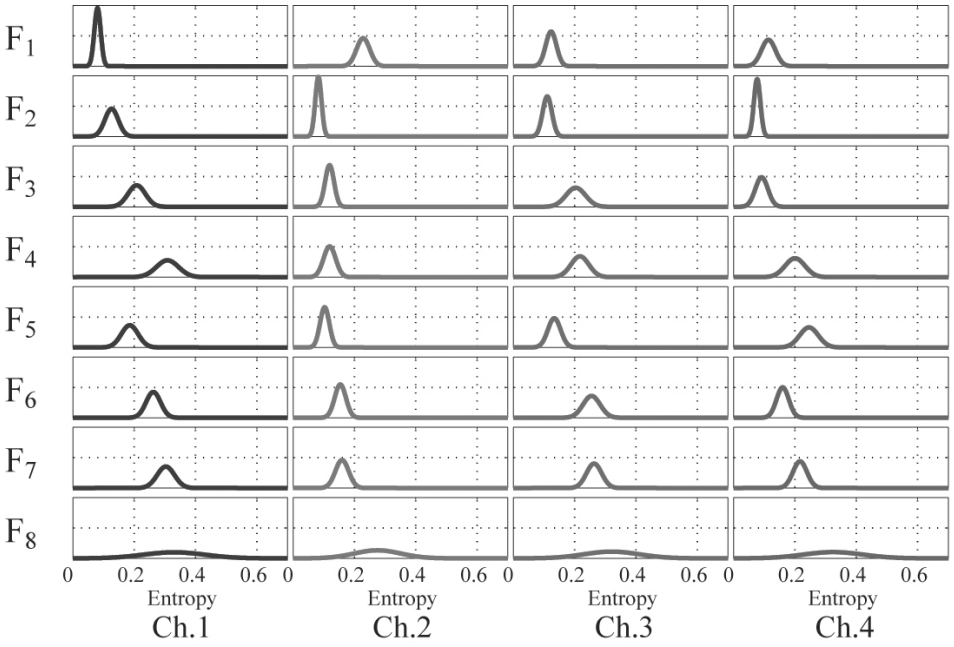

Fig. 5. Probabilistic model of entropy the EMG signals.

$$L(k)=\prod_{c=1}^{4} f_{k_c}(h). \tag{6}$$

Then, we find $\hat{k}$ which maximizes $L(k)$ such that

$$\hat{k}=\arg\max_{k} L(k) \tag{7}$$

where $\hat{k}$ means the estimated motion. Fig. 6 shows the likelihood for various candidates of finger motions.

EXPERIMENTAL RESULTS

A cross-validation is used to estimate the inference accuracies. The number of training data is 25 and that of the test data is 25. All test data are excluded from the training data. The results are averaged over 500 combinations.

The accuracy for six motions (F_1, F_2, F_3, F_4, and F_8) using the proposed method was 100.00% without any confusions as shown in Table 1. The proposed method can infer the motions more accurately than the studies of Uchida et al. (1992)

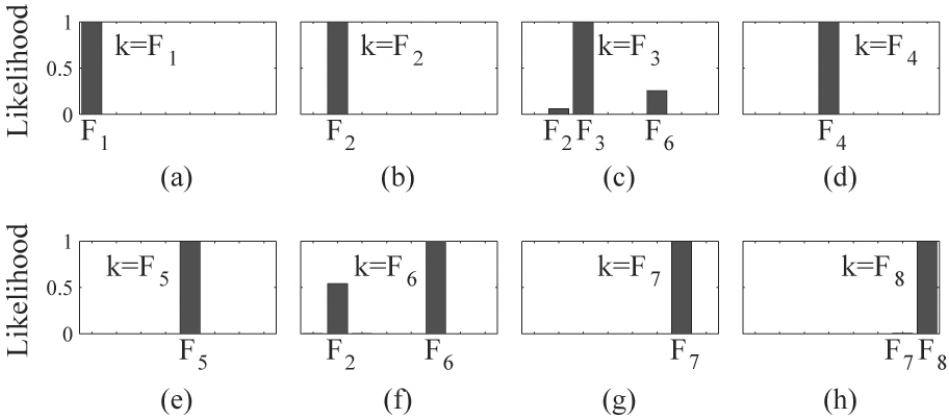

Fig. 6. Likelihood for various candidates of finger motions (each value is normalized so that the maximum was equal to one. k and $\hat{k}$ denote the actual and the inferred motions, respectively). (a) $k=F_1$, $\hat{k}=F_1$ (b) $k=F_2$, $\hat{k}=F_2$ (c) $k=F_3$, $\hat{k}=F_3$ (d) $k=F_4$, $\hat{k}=F_4$ (e) $k=F_5$, $\hat{k}=F_5$ (f) $k=F_6$, $\hat{k}=F_6$ (g) $k=F_7$, $\hat{k}=F_7$ (h) $k=F_8$, $\hat{k}=F_8$.

Table 1. Inference accuracy (%) for six motions (subject A, k: actual motion, $\hat{k}$: inferred motion)

$\hat{k}$ \ k	F_1	F_2	F_3	F_4	F_5	F_8
F_1	100%					
F_2		100%				
F_3			100%			
F_4				100%		
F_5					100%	
F_8						100%

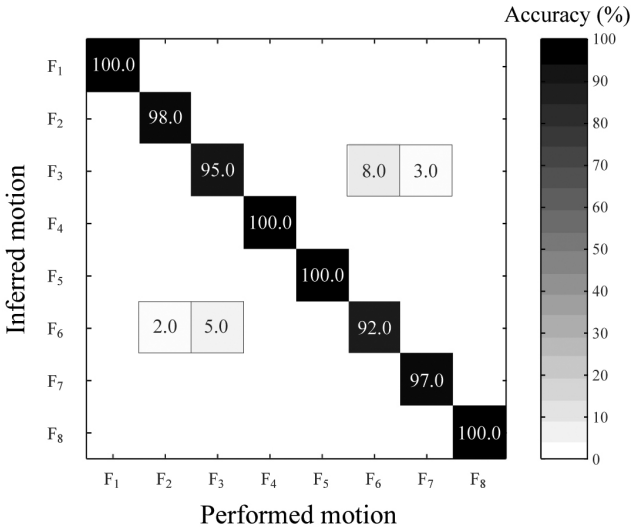

Fig. 7. Confusion matrix (subject A, test data: 25, training data: 25).

and Chen et al. (2007)

Fig. 6 shows Likelihood for various candidates of finger motions (each value is normalized so that the maximum was equal to one. k and $\hat{k}$ denote the actual and the inferred motions, respectively).

Table 2. Inference accuracy (subject A, test data: 25, training data: 25)

	Mean (%)	S.D (%)
F_1	100.0	0.00
F_2	98.0	1.41
F_3	95.0	2.20
F_4	100.0	0.00
F_5	100.0	0.00
F_6	92.0	2.74
F_7	97.0	1.72
F_8	100.0	0.00

Table 3. False table (subject A, k: actual motion, $\hat{k}$: inferred motion)

	F_2	F_3	F_6	F_7
F_3	0.0%	–	8.0±2.7%	3.0±1.7%
F_6	2.0±1.4%	5.0±2.2%	–	0.0%

(a) $k=F_1$, $\hat{k}=F_1$ (b) $k=F_2$, $\hat{k}=F_2$
(c) $k=F_3$, $\hat{k}=F_3$ (d) $k=F_4$, $\hat{k}=F_4$
(e) $k=F_5$, $\hat{k}=F_5$ (f) $k=F_6$, $\hat{k}=F_6$
(g) $k=F_7$, $\hat{k}=F_7$ (h) $k=F_8$, $\hat{k}=F_8$

The average inference accuracy for four motions (flexion of thumb, flexion of index finger, flexion of middle finger, flexion of all fingers) in a study (Uchida et al., 1992) was 86% and the accuracy for six motions (extension of thumb, extension of index finger, extension of middle finger, extension of ring finger, extension of little finger, and 'hook' gesture) was 96.83% (Chen et al., 2007).

The inference results for eight motions ($F_1 \sim F_8$) are summarized in Table 2 showing the high

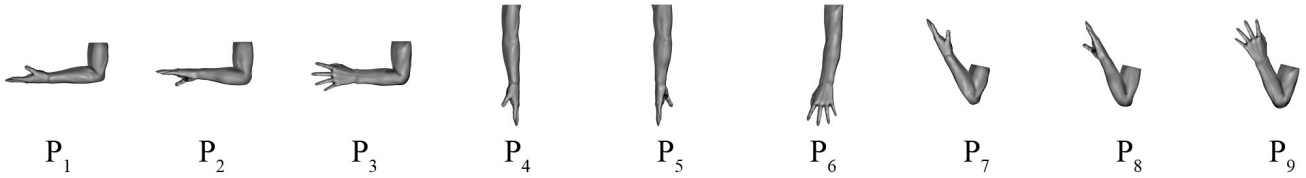

Fig. 8. Defined basic various nine postures.

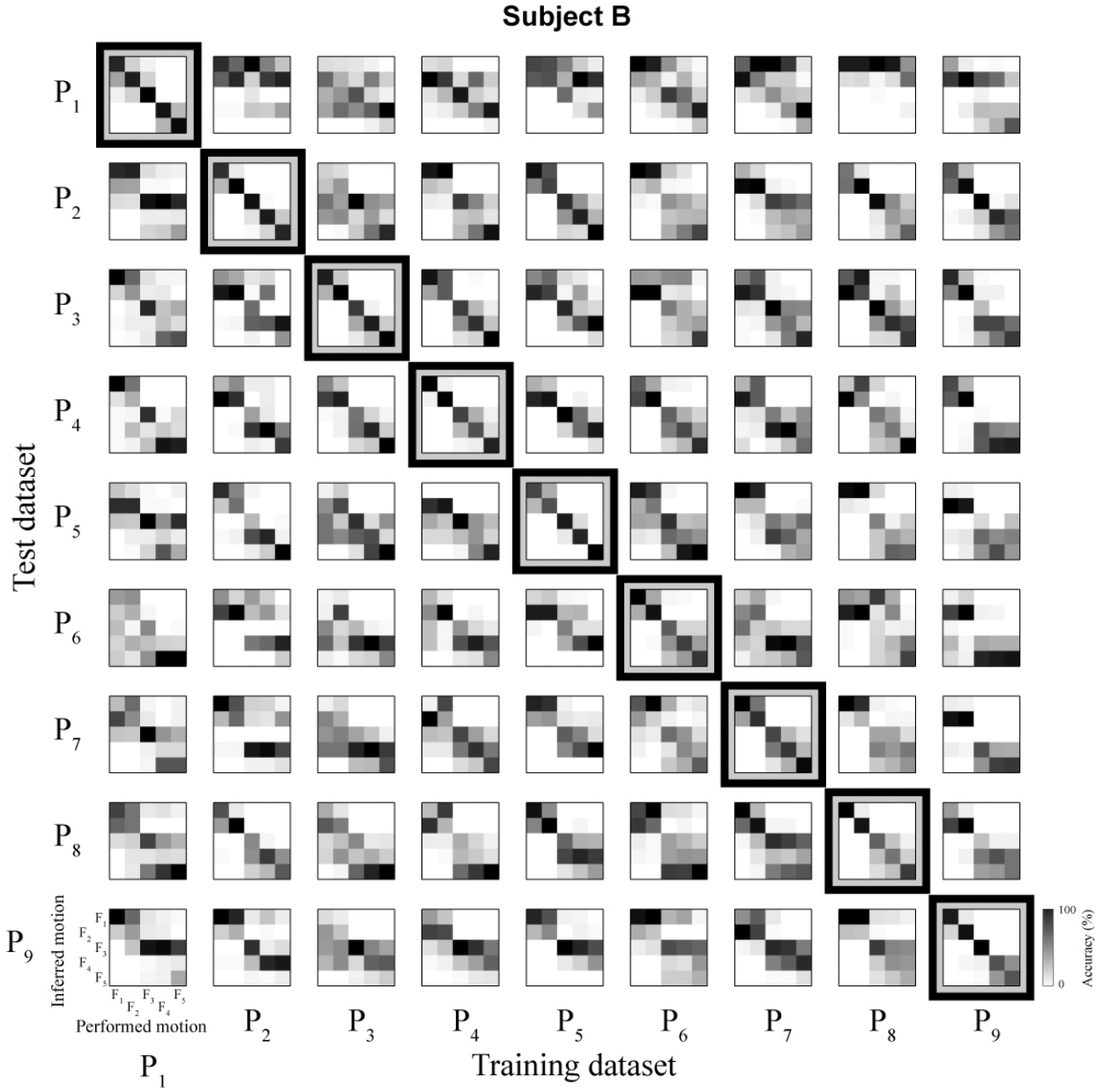

Fig. 9. Inference accuracies on various postures, $P_1 \sim P_9$ (subject B).

inference accuracy. The inference accuracies on F_1, F_4, F_5, and F_8 are 100% but the slight decreases on F_2, F_3, F_6, and F_7 arise from false inference. Fig. 7 shows the confusion matrix which visualizes the false inference among the performed motions and Table 3 shows the false inference rate which indicates the rate when performed motion is inferred incorrectly. The false inference rate on F_2

Table 4. Average Inference accuracy

Test dataset	Training dataset								
	P_1	P_2	P_3	P_4	P_5	P_6	P_7	P_8	P_9
P_1	74.72%	26.83%	27.12%	37.07%	30.45%	38.34%	27.49%	20.83%	40.83%
P_2	38.24%	83.78%	41.78%	49.20%	62.29%	43.65%	43.20%	63.49%	62.94%
P_3	53.79%	44.59%	76.22%	64.21%	43.02%	42.75%	46.85%	48.74%	54.43%
P_4	54.69%	50.54%	61.09%	81.15%	50.16%	56.67%	40.70%	45.14%	46.19%
P_5	39.58%	65.70%	41.63%	49.42%	83.60%	44.83%	42.45%	47.22%	34.72%
P_6	39.38%	37.42%	40.77%	50.85%	40.42%	62.62%	35.79%	38.02%	36.75%
P_7	41.20%	41.14%	32.22%	38.51%	42.24%	40.30%	63.07%	43.98%	39.84%
P_8	43.42%	65.82%	40.42%	35.68%	52.72%	37.87%	44.91%	76.83%	50.05%
P_9	45.33%	50.74%	36.34%	40.93%	44.00%	34.34%	37.70%	44.58%	77.55%

confused with F_6 is 2.00±1.41%. The false inference rate on F_3 confused with F_6 is 5.00±2.20% while that on F_6 confused with F_3 is 8.00±2.74%. The false inference rate on F7 confused with F_3 is 3.00±1.72%.

Influence of human arm posture

We set nine arm postures to find out how much accuracies hold down when human changes arm posture. Fig. 8 shows basic postures.

Matrices on the diagonal site in Fig. 9 show inference accuracies for five single-finger flexion motions of each posture; the number of training data was 25 and that of test data was equal. Each experiment was done 50 times. All test data were excluded from the training data. The average inference accuracies are 74.72%, 83.78%, 76.22%, 81.15%, 83.60%, 62.62%, 63.07%, 76.83%, and 77.55%, respectively.

We tested again with the data of another postures as a training dataset. Other matrices in Fig. 9 show the results. The average inference accuracies are shown in Table 4. The shaded cells indicate the maximum average accuracy in the same row and these match the diagonal cells.

Accordingly, the data of an posture is not appropriate to the reference of other postures. This fact indicates that a robust finger motion decoding method cannot be implemented without a scheme detects changes of arm's posture.

DISCUSSION

We have proposed a new method to infer finger flexing motions based on the entropy and the maximum likelihood estimation. The average recognition accuracy for six finger motions was 100.00% and the accuracy for eight finger motions was 97.75%. Also we have shown the quantitative interpretation of the need of avoidance of use of reference dataset cross arm posture because that influences the correlations between the EMG signals and the performed finger flexing motions. This study may trigger a new type of human-computer interface with user's intuitive hand motions which could control electronic devices.

ACKNOWLEDGEMENT

This research was supported by the MKE (The Ministry of Knowledge Economy), Korea, under the ITRC (Information Technology Research Center) support program supervised by the NIPA (National IT Industry Promotion Agency). (NIPA-2010-C1090-1021-0010).

REFERENCES

Capurro A, Diambra L, Lorenzo D, Macadar O, Martin MT, Mostaccio C, Plastino A, Perez J, Rofmane E, Torres ME and Velluti J (1999) Human brain dynamics: the analysis of EEG signals with Tsallis information measure. *Physica A* 265:235-254.

Chen X, Zhang X, Zhao Z, Yang J and Wang K (2007) Multiple Hand Gesture Recognition based on Surface EMG Signal. The 1st International Conference on Bioinformatics and Biomedical Engineering, Wuhan, China, 506-509.

Englehart K and Hudgins B (2003) A robust, real-time control scheme for multifunction myoelectric control, IEEE Trans. *On Biomed Eng* 50:848-854.

Englehart K, Hudgins B and Parker PA (2001) A Wavelet-Based Continuous Classification for Multifucntion Myo-

electric Control, IEEE Trans. *On Biomed Eng* 48:302-311.
Hudgins B, Parker P and Scott R (1993) A new strategy for multifunction myoelectric control, IEEE Trans. *On Biomed Eng* 40:82-94.
Martin MT Plastinob AR and Plastino A (2000) Tsallis-like information measures and the analysis of complex signals. *Physica A* 275:262-271.
Momen K, Krishnan S and Chau T (2007) Real-Time Classification of Forearm Electromyographic signals Corresponding to User-Selected Intentional Movements for Multifunction Prosthesis Control, IEEE Trans. *On Neural Systems and Rehabilitation Engineering* 15:535-542.
Nagata K, Ando K, Magatani K and Yamada M (2007) Development of the hand motion recognition system based on surface EMG using suitable measurement channels for pattern recognition. Conf. Proc. of the IEEE Trans. On Eng Med Biol Soc 5214-5217.
Nishikawa D, Yu W, Yokoi H and Kakazu Y (1999) EMG Prosthetic Hand Controller Discriminating Ten Motions using Real-time Learning Method, IEEE/RSJ Intl. Conf. On Intelligent Robots and Systems, Kyongju, South Korea 3:1592-1597.
Sabeti M, Katebi S and Boostani R (2009) Entropy and complexity measures for EEg signal classification of schizophrenic and control participants. *Artif Intell Med* 47: 263-274.
Shannon CE and Weaver W (1963) The mathematical theory of communication. University of Illinois Press, Urbana, Illinois.
Shin HC, Tong S, Yamashita S, Jia X, Geocadin RG and Thakor NV (2006) Quantitative EEG and effect of hypothermia on brain recovery after cardica arrest, IEEE Trans. *On Biomed Eng* 53:1016-1023.
Sornmo L and Laguna P (2005) *Bioelectrical signal processing in cardiac and neurological applications.* Elsevier Academic Press, London.
Tong S, Bezerianos A, Paul J, Zhu Y and Thakor N (2002) Nonextensive entropy measure of EEG following brain injury from cardiac arrest. *Physica A* 305:619-628.
Uchida N, Hiraiwa A, Sonehara N and Shimohara K (1992) EMG Pattern Recognition by Neural Networks for Multi Fingers Control. Proceedings of the Annual International Conference of the IEEE. *On Engineering in Medicine and Biology Society* 3:1016-1018.